Journal of Scientific Computing, Vol. 17, Nos. 1–4, December 2002 (© 2002)

A Semi-Lagrangian Method for Turbulence Simulations Using Mixed Spectral Discretizations

Jin Xu,[1] Dongbin Xiu,[1] and George Em Karniadakis[1,2]

Received August 31, 2001; accepted (in revised form) November 28, 2001

We present a semi-Lagrangian method for integrating the three-dimensional incompressible Navier–Stokes equations. We develop stable schemes of second-order accuracy in time and spectral accuracy in space. Specifically, we employ a spectral element (Jacobi) expansion in one direction and Fourier collocation in the other two directions. We demonstrate exponential convergence for this method, and investigate the non-monotonic behavior of the temporal error for an exact three-dimensional solution. We also present direct numerical simulations of a turbulent channel-flow, and demonstrate the stability of this approach even for marginal resolution unlike its Eulerian counterpart.

KEY WORDS: Direct numerical simulation; spectral elements; semi-Lagrangian schemes.

1. INTRODUCTION

High-order methods, especially spectral methods, are particularly effective in direct numerical simulations (DNS) of turbulent flows. However, most Navier–Stokes implementations involve semi-implicit time integration that requires unreasonable small time step sizes. For example, for a flow corresponding to Reynolds number of 10,000, the maximum allowable time step can be at least one order of magnitude smaller than the *temporal* Kolmogorov scale [21]. It can be projected that in high Reynolds number DNS there is an *uneven distribution of resolution* in space and time, with the smallest spatial scale approximately matched but with the temporal scale over-resolved by several orders of magnitude. This inefficiency of currently employed semi-implicit schemes for DNS of inhomogeneous turbulence has been recognized before, and attempts have been made to employ fully implicit schemes [3]. However, this requires Newton iterations and non-symmetric solvers that render the overall approach inefficient.

[1] Division of Applied Mathematics, Brown University, Providence, Rhode Island 02912.
[2] To whom correspondence should be addressed. E-mail: gk@cfm.brown.edu

0885-7474/02/1200-0585/0 © 2002 Plenum Publishing Corporation

Progress can be made by employing semi-Lagrangian time-discretization, which could increase significantly the maximum allowable time step while maintaining the efficiency of symmetric solvers. This approach has been introduced in the beginning of the 1980s [17], and the basic idea is to discretize the Lagrangian derivative of the solution in time instead of the Eulerian derivative. The work here is an extension of the semi-Lagrangian scheme proposed in [21] but formulated in the context of simulating turbulent flows.

The semi-Lagrangian method depends strongly on the spatial discretization. Specifically, its accuracy is particularly sensitive to the method of backward-integration of the characteristic equation as well as the interpolation scheme to evaluate the solution at departure points. This has been shown by Falcone and Ferretti [5] who conducted a rigorous analysis of the stability and convergence properties of semi-Lagrangian schemes for advection-diffusion equations. It has also been shown that the simplest semi-Lagrangian scheme with linear interpolation is equivalent to the classical first-order upwinding scheme [15], which is excessively dissipative (see [17] and [18]). A popular and effective choice for interpolation methods in previous works has been the cubic spline methods [10]; see also [2]. The idea of introducing high order characteristic methods has first been presented in [4] and it has been extended into the spectral frame in [9, 7].

An intriguing finding is that the error of semi-Lagrangian schemes in solving advection-diffusion equations *decreases* as the time step increases in a certain range of parameters, and this has initially led to some erroneous justifications [13, 14]. The analysis in [5] showed that the overall error of the semi-Lagrangian method is indeed *not* monotonic with respect to time step Δt, and, in particular, it has the form

$$\mathcal{O}\left(\Delta t^k + \frac{\Delta x^{P+1}}{\Delta t}\right)$$

where k refers to the order of backward time integration and P to the (spatial) interpolation order; similar conclusions had been reached earlier in [12]. Another interesting result was obtained by Giraldo [6], who combined the semi-Lagrangian approach with a spectral element discretization for the advection-diffusion equation. He found that for polynomial order $P \geqslant 4$ the combined scheme exhibits neither dissipation nor dispersion errors.

The extension of the semi-Lagrangian method to the solution of Navier–Stokes equations was presented in the pioneering work of Pironneau (1982) [16]. He demonstrated nonlinear stability of the method even as the viscosity approaches zero. He also obtained suboptimal error estimates, which were improved later by Süli (1988) [19]. Most of the previous analysis and numerical implementations in CFD applications have employed the Taylor–Hood finite element and are first-order in time. In a more recent paper [1],

an error analysis was conducted for the fractional-step method for incompressible Navier–Stokes equations. In particular, the pressure-correction version of the fractional scheme with first-order time-stepping was analyzed and an extension to second-order was proposed but not analyzed.

In this paper, we present a semi-Lagrangian method for simulating three-dimensional incompressible turbulent flows specifically in channel domains, extending the work in [21]. In particular, we apply a Jacobi-based spectral element discretization along the inhomogeneous direction [8] and Fourier collocation along the other two homogeneous directions, similar to [20]. We study in detail the dependence of the overall accuracy upon the time step for an exact solution of the three-dimensional Navier–Stokes equations. We then present results from a DNS of turbulence for 48^3 resolution that demonstrate the effectiveness of the method.

2. FORMULATION

2.1. Advection-Diffusion Equation

Let us first consider an advection-diffusion equation written in Eulerian form

$$\frac{\partial \phi}{\partial t} + u \cdot \nabla \phi = \nu \nabla^2 \phi \tag{1}$$

and in semi-Lagrangian form

$$\frac{d\phi}{dt} = \nu \nabla^2 \phi \tag{2}$$

Unlike Lagrangian formulations, in the semi-Lagrangian formulation the computational mesh is fixed. At each time step, a discrete set of particles arriving at the grid points is tracked backwards over a single time step along its characteristic line up to its departure points. The solution values at the departure points are then obtained by interpolation. For example, the second-order Crank–Nicolson scheme for the above equation is

$$\frac{\phi^{n+1} - \phi_d^n}{\Delta t} = \nu \nabla^2 \left(\frac{\phi^{n+1} + \phi_d^n}{2} \right), \tag{3}$$

$$\frac{dx}{dt} = u(x, t), \qquad x^{n+1} = x(t^{n+1}) = x_a \tag{4}$$

Here ϕ_d^n denotes the value of ϕ at the departure points x_d at time level n, and x_a is the position of the arrival points which coincide with the grid points. The characteristic Eq. (4) is solved backward, i.e., we solve for the departure point at time level n, x_d^n, with the initial condition $x^{n+1} = x_a$.

The departure points do not coincide with the grid points, and thus a search-interpolation procedure is needed. Also, the overall accuracy and efficiency of the semi-Lagrangian method depends critically on both the accuracy of backward integration as well as the accuracy of the interpolation method. In the following, we provide some details on how to implement both algorithms.

2.2. Backward Integration

We solve Eq. (4) for one single time step in order to obtain $x_d = x(t^n)$ by the *explicit* second-order mid-point rule

$$\hat{x} = x_a - \frac{\Delta t}{2} u(x_a, t^n), \tag{5}$$

$$x_d = x_a - \Delta t\, u\left(\hat{x}, t^n + \frac{\Delta t}{2}\right) \tag{6}$$

By defining

$$\alpha \equiv x_a - x_d$$

we can re-write the explicit mid-point rule as

$$\alpha = \Delta t\, u\left(x_a - \frac{\Delta t}{2} u(x_a, t^n), t^n + \frac{\Delta t}{2}\right) \tag{7}$$

Similarly, we employ *implicit* integration for Eq. (4) setting

$$\hat{x} = x_a - \frac{\Delta t}{2} u\left(\hat{x}, t^n + \frac{\Delta t}{2}\right)$$

to arrive at the implicit mid-point rule

$$\alpha = \Delta t\, u\left(x_a - \frac{\alpha}{2}, t^n + \frac{\Delta t}{2}\right) \tag{8}$$

This is the backward-integration algorithm used in most of previous semi-Lagrangian schemes. Although the explicit and implicit schemes are formally of second-order, a small accuracy improvement has been reported for the implicit scheme. Equation (8) has to be solved iteratively, but numerical experiments show that only a few iterations are needed for convergence (typically around five). For an advection-diffusion equation with the velocity field known analytically, the additional cost associated with the iterations is negligible. However, for a velocity field known only in numerical form, the iteration process is costly because each substep requires a

search-interpolation procedure. Our numerical results show that the two methods give almost identical results in practice, and for more general problems, especially for Navier–Stokes equations, the explicit method is preferred.

2.3. Search-Interpolation Procedure

We consider a three-dimensional channel domain with spectral elements/hp along the inhomogeneous direction and Fourier collocation along the two homogeneous directions (streamwise and spanwise). In its current implementation, we first locate in which spectral element the departure point resides and perform interpolation in modal space along all three-directions. This involves the entire Fourier expansions which is computationally expensive. Currently, we are working on an implementation that employs a more localized interpolation in the Fourier directions to reduce that cost.

2.4. Incompressible Navier–Stokes Equations

We consider the incompressible Navier–Stokes equations in Lagrangian form

$$\frac{du}{dt} = -\nabla p + \nu \nabla^2 u, \qquad \nabla \cdot u = 0 \tag{9}$$

We employ a stiffly-stable scheme to discretize the above equations [8]. A second-order time-discretization corresponds to

$$\frac{\frac{3}{2}u^{n+1} - 2u_d^n + \frac{1}{2}u_d^{n-1}}{\Delta t} = (-\nabla p + \nu \nabla^2 u)^{n+1} \tag{10}$$

where u_d^n is the velocity u at the departure point x_d^n at time level t^n, and u_d^{n-1} is the velocity at the departure point x_d^{n-1} at time level t^{n-1}. The departure point x_d^n is obtained by solving

$$\frac{dx}{dt} = u^{n+1/2}(x, t), \qquad x(t^{n+1}) = x_a$$

and also

$$u^{n+1/2} = 3/2u^n - 1/2u^{n-1}$$

The point x_d^{n-1} is obtained by solving

$$\frac{dx}{dt} = u^n(x, t), \qquad x(t^{n+1}) = x_a$$

By using the above characteristic equations, the resulting scheme is second-order accurate in time.

Specifically, for computational convenience we use the following three substeps to solve Eq. (10)

$$\frac{\hat{u}-2u_d^n+\frac{1}{2}u_d^{n-1}}{\Delta t}=0, \tag{11}$$

$$\frac{\hat{\hat{u}}-\hat{u}}{\Delta t}=-\nabla p^{n+1}, \tag{12}$$

$$\frac{\frac{3}{2}u^{n+1}-\hat{\hat{u}}}{\Delta t}=\nu\nabla^2 u^{n+1} \tag{13}$$

The discrete divergence-free condition results in a consistent Poisson equation for the pressure, i.e.

$$\nabla^2 p^{n+1}=\frac{1}{\Delta t}\nabla\cdot\hat{u}$$

with accurate pressure boundary conditions of the form [8]

$$\frac{\partial p}{\partial n}=-\nu\cdot[\hat{u}+\nabla\times\omega^{n+1}]$$

where n is the unit normal, and ω is the vorticity.

3. NUMERICAL RESULTS

3.1. Convergence Rate

We first present results from comparisons with an exact three-dimensional solution to the incompressible Navier–Stokes equations, given by

$$u=\sin(mx)\cos(ly)\cos(nz)\,e^{-t/Re}$$

$$v=-\frac{m+n}{l}\cos(mx)\sin(ly)\cos(nz)\,e^{-t/Re}$$

$$w=\cos(mx)\cos(ly)\sin(nz)\,e^{-t/Re}$$

where Re is the Reynolds number and m, l, n define the wavenumbers along the three directions. We determine the pressure $p(x, y, z, t)$ from the Navier–Stokes equations (assuming that no forcing is applied in the y-direction, i.e., $f_y=0$) to be

$$p(x, y, z, t) = -\frac{m+n}{l^2 Re}(m^2+l^2+n^2-1)\cos(mx)\cos(ly)\cos(nz)\, e^{-t/Re}$$
$$+\frac{m(m+n)}{4l^2}\sin^2(mx)\cos(2ly)\cos^2(nz)\, e^{-2t/Re}$$
$$+\frac{(m+n)^2}{4l^2}\cos^2(mx)\cos(2ly)\cos^2(nz)\, e^{-2t/Re}$$
$$+\frac{n(m+n)}{4l^2}\cos^2(mx)\cos(2ly)\sin^2(nz)\, e^{-2t/Re}$$

With this expression for pressure we can now evaluate the extra forces along the two other directions f_x and f_z, which are computed so that the above is an exact Navier–Stokes solution. The domain used was a cube of size $2\pi^3$.

We first tested that exponential convergence is realized with errors almost identical to the Eulerian approach. In Fig. 1 we plot the L_2 error for all three components of velocity for wavenumbers $m = l = n = 1$. Only one element was used along the y-direction for this solution, with P denoting the Jacobi polynomial order. Similar results hold for a multi-element discretization. Also, the number of collocation points along the two Fourier directions is set to $M = N = P$ for this case. The Reynolds number was set to $Re = 1$ and the final time of integration was $T = 1$.

The non-monotonic behavior of the temporal error obtained by the theoretical analysis for advection-diffusion equations is

$$\mathcal{O}\left(\Delta t^2 + \frac{\Delta s^{P+1}}{\Delta t}\right)$$

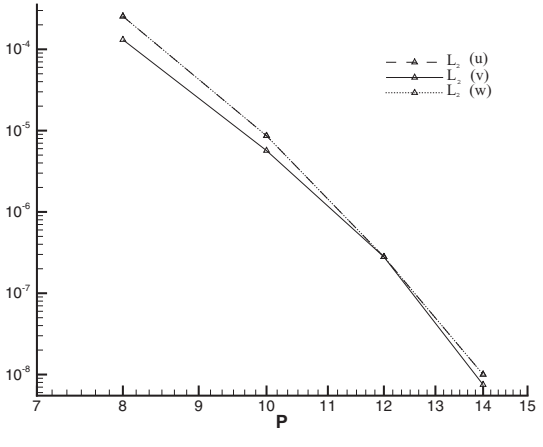

Fig. 1. Errors versus polynomial order for the exact three-dimensional solution ($Re = 1$).

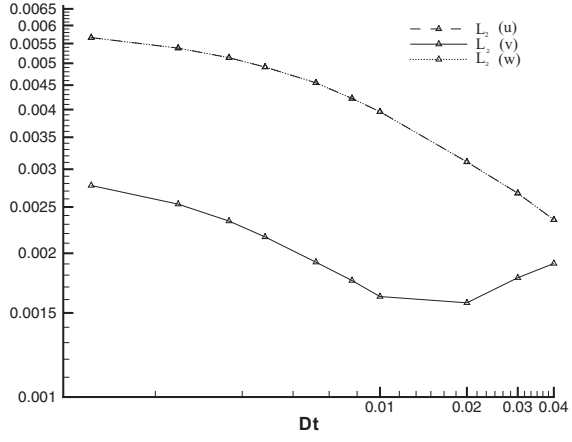

Fig. 2. Errors versus time step for the exact three-dimensional solution; resolution $P = 6 = M = N$. ($Re = 1$).

where Δs is an equivalent grid spacing. This behavior is realized in our computations of the exact Navier–Stokes solutions, as shown in Fig. 2. We note that the u and w velocity components correspond to identical curves but the normal velocity component v exhibits a different behavior. This different behavior can be attributed to the fractional stepping scheme and it is similar to the Eulerian approach. If we increase the resolution along the y-direction only from $P = 6$ to $P = 8$ (Fig. 3), we observe a large reduction in the error for all components but also a different qualitative trend. This is consistent with the aforementioned error estimate and the

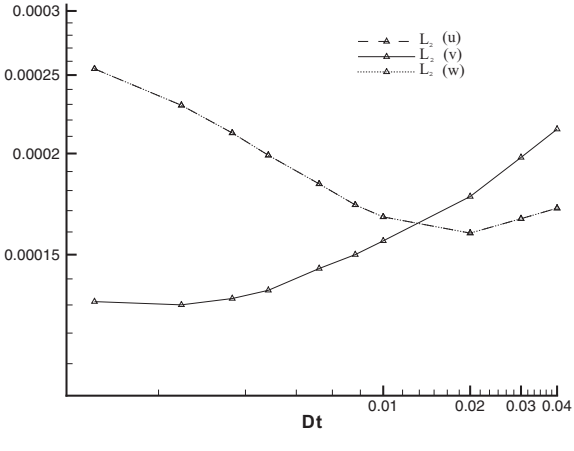

Fig. 3. Errors versus time step for the exact three-dimensional solution; resolution $P = 8$ and $M = N = 6$. ($Re = 1$).

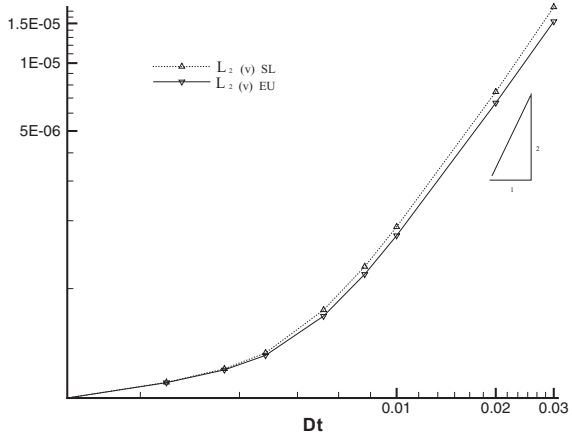

Fig. 4. Comparison of Eulerian (EU) and semi-Lagrangian schemes (SL). Errors versus time step for the exact three-dimensional solution; resolution $P = M = N = 12$. ($Re = 1$).

fact that exponential convergence is achieved. The results in both plots suggest that both error terms are comparable for this resolution.

At higher resolution, the first term in the error dominates and this behavior is similar to the one obtained in the Eulerian approach. A comparison of the two approaches is shown in Fig. 4; for the semi-Lagrangian scheme the L_2 error is slightly larger compared to the Eulerian scheme. We also see from Fig. 4 that a second-order time-accuracy is obtained. In Fig. 5 we plot the errors for Reynolds number $Re = 10^6$ and final time

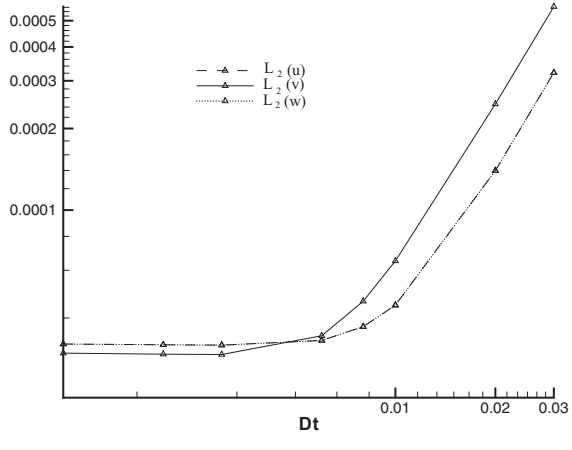

Fig. 5. Reynolds number $Re = 10^6$. Errors versus time step for the exact three-dimensional solution; resolution $P = M = N = 12$.

of integration $T = 1$. We see that the same non-monotonic behavior is obtained as in the low Reynolds number case $Re = 1$ studied in the previous figures.

3.2. DNS of Turbulent Channel-Flow

Here we perform direct numerical simulations of turbulent channel-flow in a periodic domain (in x- and z-directions) of size (x, y, z):$2\pi \times 2 \times 2\pi$. The Reynolds number based on the half-channel width and the wall shear velocity is $Re_* = 116$. We interpolated an initial turbulent 64^3 field to a 48^3 field and ran the simulation for several eddy turn-over times (50 convective units) with the de-aliased Eulerian code. We note here that the corresponding Eulerian simulation without de-aliasing was unstable even at very small time steps. We then collected statistics for $T = 5$ and $T = 20$ convective units for the Eulerian simulation; a time step of $\Delta t = 1/200$ was employed. The semi-Lagrangian simulation was performed with time step $\Delta t = 1/20$, and statistics were gathered for total time $T = 20$ convective units. Of course, no de-aliasing is required in this case. In wall units the time step used in the semi-Lagrangian method is $\Delta t^+ = \Delta t \cdot u_\tau^2 / \nu = 0.2645$, which is smaller than the Kolmogorov time scale; u_τ is the wall shear velocity. The Kolmogorov scale was estimated at $y^+ = 5$ to be $\tau_K^+ = \sqrt{u_\tau^4 / (\epsilon \nu)} \approx 0.33$ using an approximate value for the dissipation rate $\epsilon \approx 0.10$ [11]. We note here that the time Kolmogorov scale in [3] was overestimated; the value of 2.4 (in wall units) reported would correspond to a value of dissipation rate of $\epsilon \approx 0.002$ compared to about 0.16 at the wall [11].

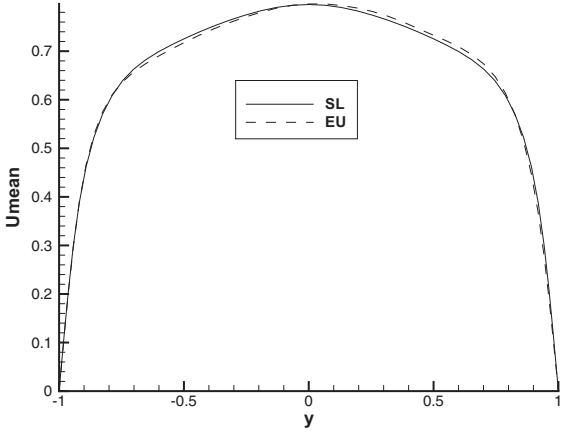

Fig. 6. Profile of mean velocity from the 48^3 DNS. The solid line corresponds to the Eulerian simulation and the dash line to the semi-Lagrangian simulation. Reynolds number $R_* = 116$.

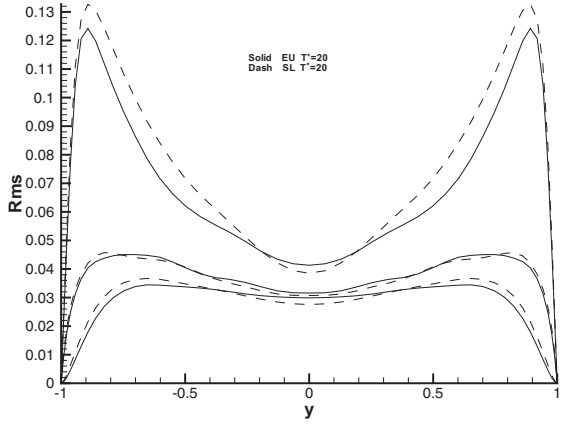

Fig. 7. Comparison of turbulence intensities from the 48^3 DNS. The solid line corresponds to the Eulerian simulation and the dash line to the semi-Lagrangian simulation. Reynolds number $R_* = 116$.

A comparison of the mean velocity profile is shown in Fig. 6; no significant differences are observed despite the very large time step employed in the semi-Lagrangian simulation. However, some differences are present in Fig. 7, where we plot the *rms* values of all three velocity components for both approaches. The more pronounced differences correspond to the streamwise turbulent intensity, which may be associated with time-averaging errors. To evaluate this we compare these profiles obtained by averaging

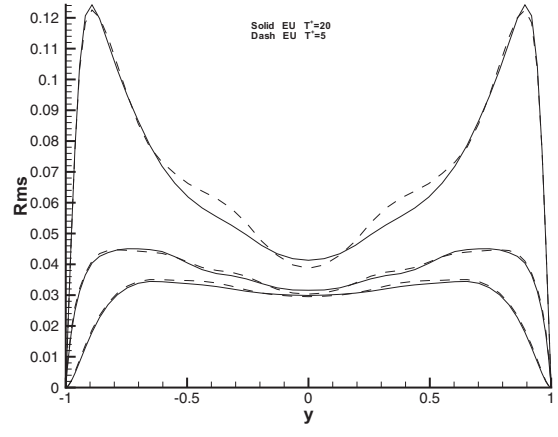

Fig. 8. Comparison of turbulence intensities from the Eulerian 48^3 DNS. The solid line corresponds to averaging over $T = 20$ and the dash line to averaging over $T = 5$; Reynolds number $R_* = 116$.

also over $T = 5$ and we, indeed, obtain noticeable differences as shown in Fig. 8.

4. SUMMARY

We have developed a spectral semi-Lagrangian algorithm for simulating turbulent channel flow, and have demonstrated its accuracy and its stability. The overall error is comparable to the Eulerian scheme but the stability is greatly enhanced. However, in its current implementation the method employs global interpolation, which makes it computationally very expensive. Specifically, the method is approximately ten times slower than the Eulerian method for the 48^3 simulation presented, so with the gain factor of ten (for the semi-Lagrangian) in the time step, the overall simulation cost is the same for both methods. Better local interpolation procedures need to be implemented that do not compromise accuracy while providing a speed-up factor that will make this method more efficient than the Eulerian approach for DNS of turbulence. This has been done in the context of fully three-dimensional geometries, where hexahedra and tetrahedra spectral/*hp* elements form a natural framework for local Lagrangian interpolation [21]. In that case a speed-up factor of about five (on average) was achieved in favor of the semi-Lagrangian method. A similar domain decomposition scheme should also be adopted for the channel geometry; we will report such work as well as practical high Reynolds number DNS in future publications.

ACKNOWLEDGMENTS

This work was supported by DARPA. Computations were performed at Brown's TCASCV, and also at NPACI's and NCSA's facilities supported by NSF.

REFERENCES

1. Achdou, Y., and Guermond, J. L. (2000). Convergence analysis of a finite element projection/Lagrange–Galerkin method for the incompressible Navier–Stokes equations. *SIAM J. Numer. Anal.* **37**, 799.
2. Bartello, P., and Thomas, S. J. (1996). The cost-effectiveness of semi-Lagrangian advection. *Mon. Wea. Rev.* **124**, 2883.
3. Choi, H., and Moin, P. (1994). Effects of computational time step on numerical solutions of turbulent flow. *J. Comp. Phys.* **113**, 1.
4. Ewing, R. E., and Russel, T. F. (1981). Multistep Galerkin method along characteristics for convection-diffusion problems. In Vichnevetschy, T., and Stepleman, R. S. (eds.), *In Advances in Computational Methods for P.D.E.*, Vol. 28.
5. Falcone, M., and Ferretti, R. (1998). Convergence analysis for a class of high-order semi-Lagrangian advection schemes. *SIAM J. Numer. Anal.* **35**, 909.
6. Giraldo, F. X. (1998). The Lagrange–Galerkin spectral element method on unstructured quadrilateral grids. *J. Comput. Phys.* **147**, 114.

7. Ho, L. W., Maday, Y., Patera, A. T., and Ronquist, E. M. (1989). A high order Lagrangian-decoupling method for the incompressible Navier–Stokes equations. In Canuto, C., and Quarteroni, A. (eds.), *Proceedings of ICOSAHOM '89 Conference*, Vol. 65, North Holland.
8. Karniadakis, G. E., and Sherwin, S. J. (1999). *Spectral/hp Element Methods for CFD, Oxford University Press, London.*
9. Maday, Y., Patera, A. T., and Ronquist, E. M. (1990). An operator integration factor splitting method for time dependent problems; Application to incompressible fluid flows. *J. Sci. Comp.* **5**.
10. Malevsky, A. V. (1996). Spline-characteristic method for simulation of convective turbulence. *J. Comput. Phys.* **123**, 466.
11. Mansour, N. N., Kim, J., and Moin, P. (1988). Reynolds-stress and dissipation-rate budgets in a turbulent channel flow. *J. Fluid Mech.* **194**, 15.
12. McDonald, A. (1984). Accuracy of multi-upstream, semi-Lagrangian advective schemes. *Mon. Wea. Rev.* **112**, 1267.
13. McDonald, A., and Bates, J. R., (1987). Improving the estimate of the departure point position in a two-time level semi-Lagrangian and semi-Implicit scheme. *Mon. Wea. Rev.* **115**, 737.
14. McGregor, J. L. (1993). Economical determination of departure points for semi-Lagrangian models. *Mon. Wea. Rev.* **121**, 221.
15. Oliveira, A., and Baptista, A. M. (1995). A comparison of integration and interpolation Eulerian-Lagrangian methods. *Int. J. Numer. Methods Fluids* **21**, 183.
16. Pironneau, O. (1982). On the transport-diffusion algorithm and its applications to the Navier–Stokes equations. *Numer. Math.* **38**, 309.
17. Robert, A. (1981). A stable numerical integration scheme for the primitive meteorological equations. *Atmos. Ocean.* **19**, 35.
18. Staniforth A., and Côté, J. (1991). Semi-Lagrangian integration schemes for atmospheric models–A review. *Mon. Wea. Rev.* **119**, 2206.
19. Süli, E. (1988). Convergence and nonlinear stability of the Lagrange–Galerkin method for the Navier–Stokes equations. *Numer. Math.* **53**, 459.
20. Süli, E., and Ware, A. (1991). A spectral method of characteristics for hyperbolic problems. *SIAM J. Numer. Anal.* **28**, 423.
21. Xiu, D., and Karniadakis, G. E. (2001). A semi-Lagrangian high-order method for Navier–Stokes equations. *J. Comp. Phys.*, **172**, 658.